

Body-worn Fully-Passive Wireless Analog Sensors for Physiological Signal Capture Through Load Modulation using Resistive Transducers

Sergi Consul-Pacareu, *Student Member IEEE, EMBS*, David Arellano, and Bashir I. Morshed, *Member IEEE, EMBS*

Abstract—Fully-passive wireless body-sensors pose viable solutions for unobtrusive monitoring of physiological signals at natural settings. While fully-passive capacitive analog passive wireless sensors has been reported, we present an alternative solution with resistive based transducers. The passive sensor is composed of a loop antenna, a tuning capacitor, and a resistive transducer suitable for the type of physiological signals to be measured. The scanner transmits carrier RF signal at 13.75MHz whose amplitude is modulated based on the resistive loading by the transducer. The load modulation is captured with the signal analyzer. The system was characterized for various resistive loads of 1.2Ω to $82\text{K}\Omega$ and open at 5, 10, 20, and 40 mm co-axial distances between the transmitter and the receiver antennas. We demonstrate the practicality of the system by measuring several physiological signals like heart rate, temperature, and pulse oximetry. The wireless power used for remote sensing is very low (-20dBm , except pulse oximetry requires 0dBm). The results show the potential of developing a new set of body-worn fully-passive sensors for physiological signal monitoring.

I. INTRODUCTION

For large numbers of multimodal distributed sensors, wired sensors eventually becomes complex and unmanageable, leading to ineffective solutions. Traditional wireless sensors are not effective due to the requirement of battery, size and usability. Fully-passive sensors has the potential to be body-worn and collect physiological signals unobtrusively [4], [5]. Fully-passive sensors can be classified in two categories: wireless digital passive sensor (WDPS) and wireless analog passive sensor (WAPS). WDPS contains an ASIC chip that receives power from the scanner, turns on the circuitry and wirelessly retransmits the digital identification code or digitized signal. WDPS can collect analog signals by sampling the analog data with data acquisition chips [1], [13]. On the contrary, WAPS does not contain any digital ASIC chip, rather transmits analog signals. WAPS based on varactor and Surface Acoustic Wave (SAW) resonator has been demonstrated for various remote signal capture [8], [9], [10], [12]. These WAPS uses LC resonators with modulation based on captive changes, resulting in a shift of the resonance frequency based on the captured signals [10], [12]. For delayed backscattering, a SAW delay line to retransmit the modulated backscattered signal [9], [2].

In this paper, we demonstrate the feasibility of a novel resistive based WAPS. This passive sensor is an RLC res-

onator with damping (Q). Thus, the variation of the resistive load changes the damping factor, which can be captured from the scanner as load modulation of carrier amplitude. The advantage of a resistive based transducer is that the passive circuit is very simple, low cost and component count, thus inexpensive and can be disposable. The resistive WAPS operates in a narrow bandwidth (BW) allowing simultaneous access of large number of sensors using Frequency Division Multiple access (FDMA) as depicted in Figure 1.

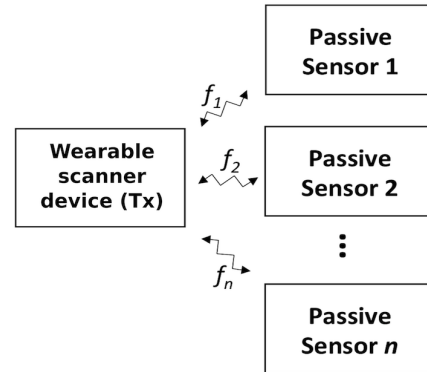


Fig. 1. System diagram of the resistive WAPS for access of multiple physiological signals using frequency multiplexing.

II. HARDWARE DESCRIPTION

For prototype development, two identical sized boards has been designed Cadence PSPICE tool (Cadence Design Systems, Inc., San Jose, CA, USA). Figure 2 shows the schematic for the scanner device and Figure 3 shows that of the passive sensor. The antenna design was based on the designs from [3].

The scanner board has two SMA connectors, one for the carrier input V_1 , which oscillates at 13.75MHz , and the other one for the signal analyzer. Two capacitors ($C_1||C_2$) are used to match the antenna to 50Ω . Another two capacitors ($C_3||C_4$) are used to adjust the resonant frequency with the loop antenna (L_1) as a planar inductor. The damping resistor (R_1) is used to lower Q.

The passive sensor has a matching coil (L_2) and two capacitors ($C_5||C_6$) to tune the antenna at the resonant frequency. The resistive load (R_L) represents the transducer that converts any physical signal to a correlated resistance value. The component values and the resonance frequencies were measured using an Agilent 4294A Impedance Analyzer (Agilent Technologies Inc., Santa Clara, CA, USA).

This work was supported by FedEx Institute of Technology Grant Number: 2013-537908

S. Consul-Pacareu, D. Arellano, and B. I. Morshed are with the Electrical and Computer Engineering Department, The University of Memphis, Memphis, TN 38152 USA. scpacareu@memphis.edu drellano@memphis.edu bmorshed@memphis.edu

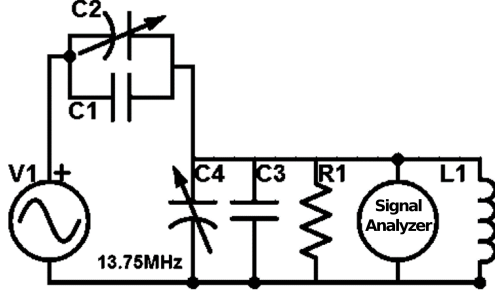


Fig. 2. Schematic of the interrogator. $C_1 = 10pF$, $C_2 = C_4 = [6 - 30]pF$, $C_3 = 200pF$, $L_1 = 635nH$, and $R_1 = 10K\Omega$.

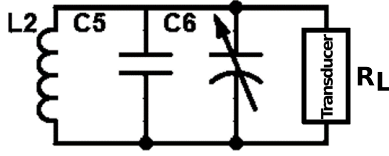


Fig. 3. Schematic of the passive sensor. $C_5 = [6 - 30]pF$, $C_6 = 200pF$, $L_2 = 635nH$.

Printed Circuit Boards (PCBs) were designed using Cadence Allegro SPB 16.6 (Cadence Design Systems, Inc., San Jose, CA, USA). The sensor and scanner board are of identical size measuring $6.89\text{ cm} \times 4.19\text{ cm}$. The PCBs were fabricated by Advanced Circuits (Aurora, CO, USA). The populated sensor and scanner device weigh $9.07g$ and $11.75g$, respectively. The test fixture kept the sensor and the scanner boards in parallel at co-axial positions (Figure 4).

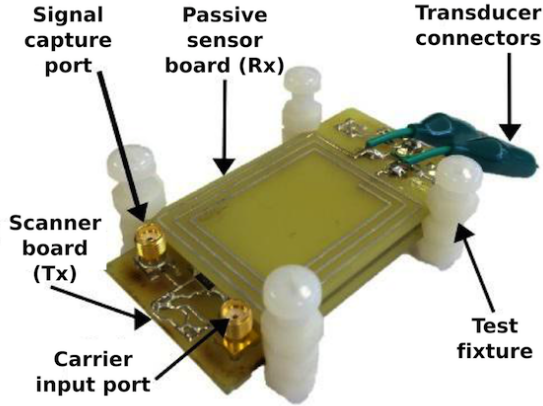


Fig. 4. The test setup for the scanner and the sensor at a co-axial parallel position where separation can be altered.

III. METHOD

The passive sensor has no power source; instead it uses the incident power signal from the scanner to modulate the loading in amplitudes as its response. The scanner power

field can also be used to provide the necessary biasing voltages to drive LEDs, which was needed for pulse oximetry measurement.

In order to measure the reflected signal, the receiver can either use a directional coupler so the reflected signal can be redirected to the acquisition system, or it can be measured at the coil terminations, measuring the loading effect by the acquisition system due to difference in impedance seen in the primary induced by the secondary coil.

From the passive sensor side, secondary coil impedance is equal to Eq.1.

$$Z_{Sensor}(w) = \left(jwL_2 \parallel \left(\frac{1}{jw(C_5 + C_6)} \right) \parallel R_L \right) \quad (1)$$

From the primary, for a mutual inductance of M , the secondary can be seen as following [12]:

$$X_{Sensor}(w) = \left(\frac{(wM)^2}{Z_{Sensor}(w)} \right) \quad (2)$$

Thus, the impedance encountered by the signal analyzer is:

$$Z_{Rec}(w) = \left(X_{Sensor}(w) + jwL_1 \parallel \frac{1}{jw(C_4 + C_3 + C_2 + C_1)} \parallel R_1 \right) \quad (3)$$

Eq.3 shows that a change in resistive load in the secondary creates a change in the received signal amplitude.

The scanner and the passive sensor maintained a separation distance of 5 to 40 mm at co-axial position for all measurements by using the testing fixture as shown in Figure 4. A DSA1030-TG3 (Rigol Technologies Inc., Beijing, China) spectrum analyzer is used to measure the frequency domain reflected signal from the sensor. The tracking generator is used to sweep from $11.5MHz$ to $15.5MHz$ with $-20dBm$ normalized output power, with settings of $RBW = VBW = 1KHz$, Gauss Filter and Positive Max Detector.

For all temporal signal measurements, the same setup as in Fig.4 is used. However, for these measurements a DG4062 (Rigol Technologies Inc., Beijing, China) signal generator is used to synthesize a tone carrier at $13.75MHz$ with $-20dBm$ of power to interrogate the passive sensors, except for the pulse oximetry, which used a higher power of $0dBm$ since an LED needs to be forward biased. The output was connected to a DSO-X 2024A (Agilent Technologies Inc., Santa Clara, CA, USA) Oscilloscope, with settings of AC coupled, $1mV/div$, Peak Detect as acquisition mode, and ASCII X-Y as output option.

IV. RESULTS

A. Impedance Range

In order to determine the working range of the system, a RS-200 (IET Labs Inc., Roslyn Heights, NY 11577 USA) calibrated resistance box was used to sweep. The parasitic capacitance and inductance between decades is removed to not affect the measurements. Figure 5 to Figure 8 show the

system responses with different resistive loads at various co-axial distances between the scanner and the passive sensor coils. For a high loads (beyond $80\text{ K}\Omega$), the response is difficult to measure since it is in parallel with $L_2||C_5||C_6$, as shown Figure 3, which has a low impedance magnitude. Similarly, the load resistance below $1\text{ K}\Omega$ is also not suitable. Also, the response sensitivity and BW reduces with greater distances.

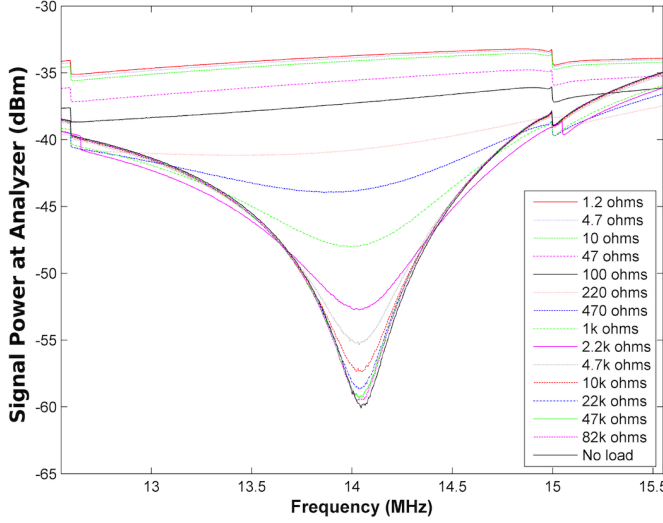


Fig. 5. Power vs frequency plot for resistive loads at 5 mm co-axial distance.

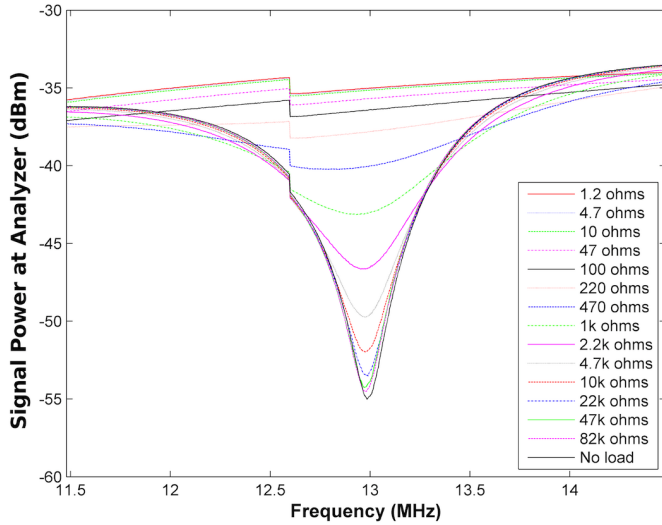


Fig. 6. Power vs frequency plot for resistive loads at 10 mm co-axial distance.

B. Heart Beat Rate

Heart beat rate signal was measured using a FSR402 (Interlink Electronics Inc., Camarillo, CA, USA) Component Of-The-Shelf (COTS) pressure transducer. The passive sensor was located in the anterior wrist, on top of the radial artery and attached to a rigid wristband to allow compression on the sensor due to blood flow expansion. Figure 9 shows

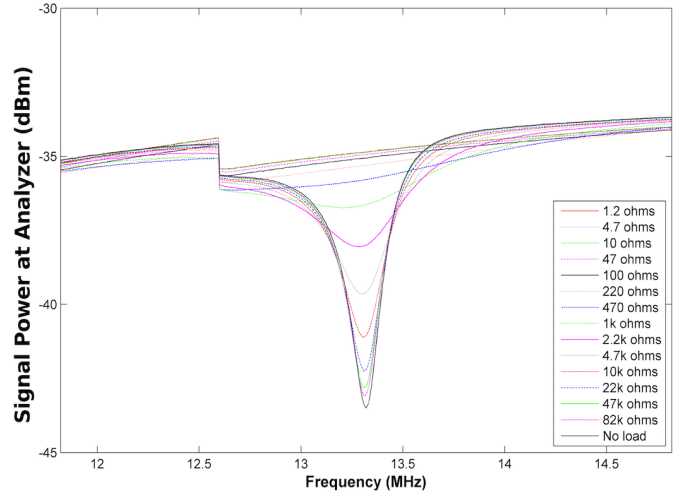


Fig. 7. Power vs frequency plot for resistive loads at 20 mm co-axial distance.

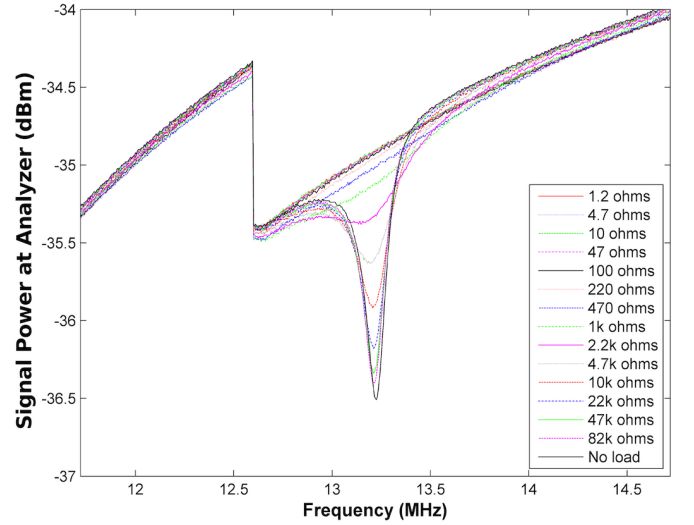


Fig. 8. Power vs frequency plot for resistive loads at 40 mm co-axial distance.

the envelope (both positive and negative sides) of the modulated signal that correlates with the heart rate. The measured rate was 60 BPM while the CMS-50DL finger pulse meter (Contec Medical Systems) provided average rate of 62 BPM.

C. Temperature

A COTS Negative Thermal Coefficient (NTC) Thermistor, NTC-503k (Jameco Electronics, Belmont, CA 94002 USA) was used to measure skin temperature. The sensor ranges from $R_{25^{\circ}\text{C}} = 50\text{ K}\Omega$ to $R_{85^{\circ}\text{C}} = 10\text{ K}\Omega$. To sweep the temperature the passive sensor was attached to a large thermal mass copper plate that was heated with a hot air gun up to 85°C and it was then allowed to naturally cool. A thermocouple probe connected to a Fluke 87A (Fluke Corp. Everett, WA, USA) was used to correlated temperature to passive sensor output. The envelope response (only positive side) from 47°C to 34°C as shown in Figure 10 depicts almost linear relationship.

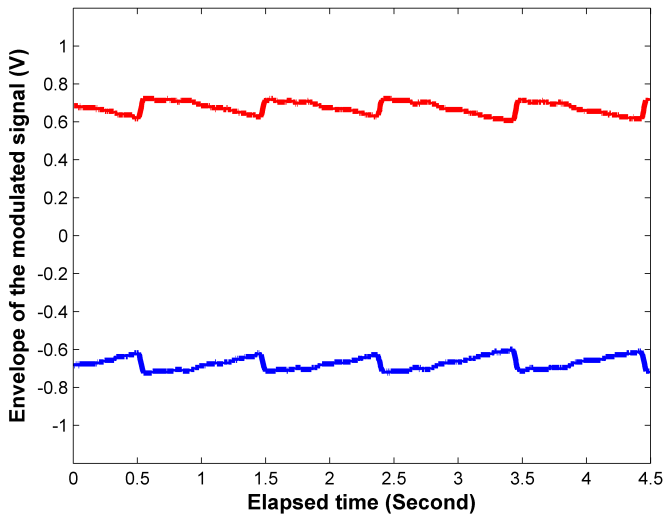


Fig. 9. Heart beat rate signal measured via WAPS with a COTS pressure transducer (showing both positive and negative sides of the modulated signal).

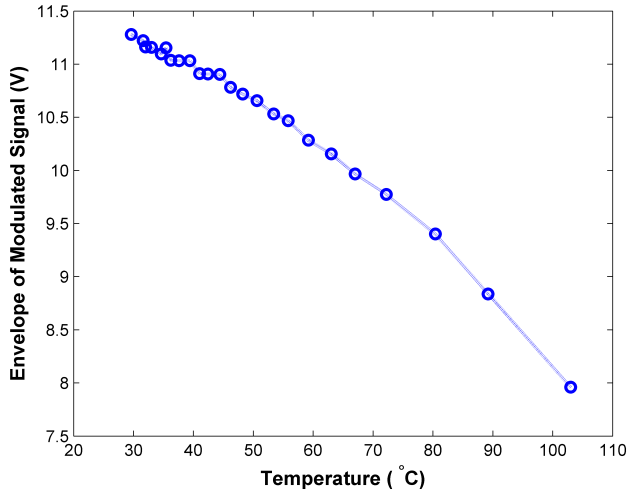


Fig. 10. Temperature measurement using a NTC Thermistor shows almost linear correlation.

D. Pulse Oximetry

Pulse oximetry is used to measure the oxygen saturation (SpO_2) non-invasively, by the detection of Hemoglobin (HbO_2) and Deoxyhemoglobin (Hb) absorption of light. With our system HbO_2 is measured with a COTS 660nm LED (red). To show the feasibility of this measurement, a COTS Light-Dependent Resistor (LDR), GL5528 was used as transducer, measurements ranging from $3K\Omega$ to $4K\Omega$. A red LED (660nm) was located at the tip of the finger while the LDR on the fingernail in opposite side. Figure 11 shows the measured readings which can be used for pulse oximetry calculation with the corresponding IR measurement.

V. CONCLUSIONS

In this paper, we introduce a new WAPS that uses resistive transducers. The system successfully used amplitude modulation of the backscattered signal to transmit information

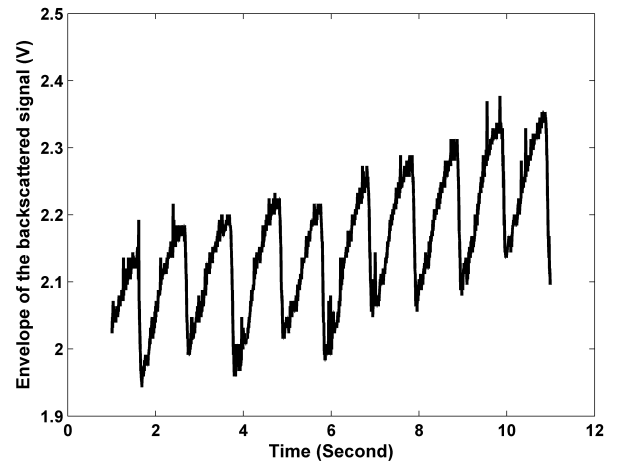


Fig. 11. Signals for pulse oximetry using a red LED-LDR pair.

when the transducer impedance is in between $1 K\Omega$ and $50 K\Omega$. We demonstrate the feasibility of physiological signal capture by probing heart beat rate, temperature, and pulse oximetry. Using a wireless passive system that uses as low power as $-20dBm$ to perform the measurements and inductive coupling, the system is specifically suitable for body-worn sensors. The results show the potential of developing the a body-worn sensor network with multiple passive sensors accessed simultaneously using frequency multiplexing technique.

REFERENCES

- [1] M. Sawan, Y. Hu, and J. Coulombe, "Wireless smart implants dedicated to multichannel monitoring and microstimulation," *IEEE Circuits and Systems Magazine*, vol. 5, no. 1, pp. 21-39, 2005.
- [2] W. Luo, Q. Fu, J. Deng, G. Yan, D. Zhou, S. Gong, Y. Hu, "An integrated passive impedance-loaded SAW sensor," *Sensors and Actuators B: Chemical*, vol. 187, pp. 215-220, 2013.
- [3] J. A. Goulbourne, "HF Antenna Cookbook", Texas Instruments, 2001.
- [4] Y. M. Chi, T. Jung, and G. Cauwenberghs, Dry-contact and noncontact biopotential electrodes: methodological review, *IEEE Reviews in Biomedical Engineering*, vol. 3, pp. 106-119, 2010.
- [5] A. Sabban, Comprehensive study of printed antennas on human body for medical applications, *Intl J Adv Med Sci*, vol. 1, pp. 1-10, 2013.
- [6] K. Finkenzeller, *The RFID Handbook*, John Wiley and Sons, 2003.
- [7] A. Dementyev, and J. R. Smith, A wearable UHF RFID-based EEG system, *IEEE Intl. Conf. RFID*, pp. 1-7, 2013.
- [8] Z. Popovic, E.A. Falkenstein, D. Costinett, and R. Zane, Low-power far-field wireless powering for wireless sensors, *Proc. IEEE*, vol. 101, no. 6, pp. 1397-1409, 2013.
- [9] W. Luo, Q. Fu, J. Deng, G. Yan, D. Zhou, S. Gong, Y. Hu, An integrated passive impedance-loaded SAW sensor, *Sensors and Actuators B: Chemical*, vol. 187, pp. 215-220, 2013.
- [10] H.N. Schwerdt, W. Xu, S. Shekhar, A. Abbaspour-Tamijani, B.C. Towe, F.A. Miranda, and J. Chae, A fully-passive wireless microsystem for recording of neuropotentials using RF backscattering methods, *J. Microelectromech Syst.*, vol. 20, no. 5, pp. 1119-1130, 2011.
- [11] H.N. Schwerdt, F.A. Miranda, and J. Chae, Analysis of electromagnetic fields induced in operation of a wireless fully passive backscattering neurorecording microsystems in emulated human head tissue, *IEEE Trans Microwave Theory and Techniques*, vol. 61, no. 5, pp. 2170-2176, 2013.
- [12] J. Riistama, E. Aittokallio, J. Verho, and J. Lekkala, Totally passive wireless biopotential measurement sensor by utilizing inductively coupled resonance circuits, *Sensors and Actuators A*, vol. 157, pp. 313-321, 2010.
- [13] R. Bashirullah, Wireless implants, *IEEE Microwave Magazine*, pp. S14-S23, Dec. 2010.